

Broad-Band Dielectric Spectroscopy on a Set of Combined Main-Chain Side-Group Liquid-Crystalline Polymers[†]

F. Kremer,* S. U. Vallerien, R. Zentel,[‡] and H. Kapitza[‡]

Max-Planck Institut für Polymerforschung, Postfach 3148, D-6500 Mainz, FRG.

Received December 2, 1988; Revised Manuscript Received March 16, 1989

ABSTRACT: Broad-band dielectric spectroscopy (10^{-1} – 10^7 Hz) was used to analyze the molecular dynamics of a set of combined main-chain side-group liquid-crystalline polymers. By varying the chemical structure, a detailed assignment of the observed relaxational processes was possible. Three relaxational processes were found: (i) an α -relaxation, which is assigned to the dynamic glass process of the polymeric main chain and through spacer coupled side-group movements, (ii) a β -relaxation, which is assigned to the rotation of the mesogenic side group around its long axis; (iii) a β_m -relaxation, which is assigned to the rotation of the mesogenic group in the main chain around its long axis.

Introduction

Combining the features of liquid-crystal main-chain and side-group polymers led Ringsdorf and Reck in 1984 to the new class of combined main-chain and side-group polymers.¹ Besides numerous papers on the molecular dynamics in other types of liquid-crystalline polymers,^{3–12} up to now only one study has been published on the molecular dynamics in this new class of liquid-crystalline polymers.² By use of dielectric spectroscopy in addition to a high-temperature relaxation, two low temperature processes were found. A detailed assignment of the two latter relaxations was not possible. For this paper 24 of these new substances with systematically varied chemical structure were available. From these, nine were selected, having appropriate dipole moments in the mesogenic group of the main chain and/or the side group. This made a detailed analysis of the molecular dynamics in this new class of liquid-crystalline polymers possible by using broadband dielectric spectroscopy.

Experimental Section

Preparation and characterization of the nine measured, combined main-chain side-group liquid-crystal polymers (see Table I and Figure 1) are described in detail in ref 13. The molecular weights were determined by GPC in CHCl_3 . Polystyrene served as the standard. The phase-transition temperatures were determined by DSC measurements and polarizing microscopy. The phase identification was done by X-ray measurements. The dielectric measurements covered the frequency range from 10^{-1} to 10^7 Hz, using a Hewlett-Packard impedance analyzer (HP-4192A, frequency range 10 – 10^7 Hz) and a frequency response analyzer (Solartron-Schlumberger FRA 1254, frequency range from 10^{-4} to 6×10^4 Hz). The latter was accomplished with a high-impedance preamplifier of variable gain.¹⁴ The nitrogen gas stream heating system covered the temperature range from 100 to 450 K; the stability of the temperature adjustment was ± 0.02 K. Both measurement systems were fully computer-controlled. The liquid-crystal sample was kept between two gold-plated brass electrodes (sample area, 314 mm^2) with a separation of $200 \mu\text{m}$, being maintained by a fused silica spacer ring. To ensure that the sample was bubble-free and filled the sample condenser totally, a custom made temperature-controlled vacuum chamber was constructed (Figure 2). It allowed the sample, which was usually obtained in powder form, to warm up above the glass transition temperature while applying a well-defined vacuum. During that process of degassing the sample, the upper electrode was not in contact with the material under study. When the sample began to melt and became homogeneously distributed in the sample area

(which was limited by the fixed silica spacer ring) the upper electrode was brought into contact with the substance by use of a vacuum-tight micrometer drive. Afterward the sample was slowly cooled down to room temperature and the vacuum was removed. Additionally this vacuum chamber allowed the experimenter to regain nearly the full amount of sample material after the measurement.

Results and Discussion

The nine liquid-crystal polymers with systematically varied chemical structures (Table I) can be separated into two different groups (for nomenclature, see ref 13). Polymers 29, 31, 37, and 39 have a low glass transition temperature; polymers 32, 40, 41, 43, and 44 have a crystalline/liquid-crystalline (lc) phase transition at higher temperatures. The crystalline state might be in some cases a highly ordered smectic phase (e.g., S_C^*).¹³ Two typical examples will be discussed in detail.

Polymer 29 (g 12 s 37 i). For polymer 29 with the 3-bromobiphenyl group as the mesogenic group both in the main chain as well as in the side group the dielectric loss ϵ'' versus temperature and frequency is shown in Figure 3. Besides the asymmetric low-temperature process, a strong relaxation at higher temperatures can be seen. The frequency dependence of the latter is shown for temperatures between 294 and 340 K (Figure 4) in order to demonstrate the quantitative analysis. For that the empirical Havriliak–Negami function¹⁵ was used:

$$\epsilon(\omega) = \epsilon_\infty + \frac{\epsilon_s - \epsilon_\infty}{(1 + (i\omega\tau)^{1-\alpha})^\beta} \quad (1)$$

where ϵ_∞ and ϵ_s are the values of the complex dielectric function on the high-frequency and low-frequency side of the relaxation process, respectively, τ is the mean relaxation time, and the two parameters α and β are fit parameters to describe the broadening and asymmetry of the relaxation time distribution. From the Havriliak–Negami function, the mean relaxation time τ and the mean relaxation rate $\nu_\tau = 1/\tau$ were reduced (Table II). In Figure 5 the mean relaxation rate ν_τ versus inverse temperature (activation plot) is shown. The experimental values can be fitted with the WLF equation¹⁶

$$\log \frac{\tau_T}{\tau_{T_g}} = \frac{-c_1(T - T_g)}{c_2 + T - T_g} \quad (2)$$

τ_T is the mean relaxation time at the temperature T , whereas τ_{T_g} is the mean relaxation time at the DSC-determined glass-transition temperature T_g . c_1 and c_2 are constants. The solid line was calculated from the WLF equation by using the parameters $\log \tau_{T_g} = -1.99$, $c_1 = 13.6$,

[†] Dedicated to Prof. Dr. E. W. Fischer on the occasion of his 60th birthday.

[‡] Present address: Institut für Organische Chemie, Universität Mainz, J.J. Becherweg 18-20, D-6500 Mainz, FRG.

Table I
Nomenclature of the Observed Nine Polymers (according to Reference 13), Phase Behavior, and Molecular Weights

side-group mesogen	main-chain mesogen					
	polymer	phase behavior	MW	polymer	phase behavior	MW
	29	g 12 s 37 i	30 900		31 g 12 s 53 n* 91 i	20 900
	37	g 17 S 90 n* 96 i	23 400		39 g 20 S _A 108 n* 144 i	28 200
	41	k 59 s _c * 105 i	39 800		43 k 63 s _c * 124 n* 133 i	39 800
					44 k ₁ 151 k ₂ 154 i	56 600

Table II
Some of the Havriliak-Negami Parameters Evaluated by Fitting the Relaxation Processes

	temp, K	H-N parameters			τ , s
		$\Delta\epsilon$	α	β	
Polymer 29					
β_s -process	207.34	0.44	0.52	0.43	7×10^{-6}
	170.29	0.45	0.40	0.43	1×10^{-3}
α -process	313.22	3.26	0.63	0.51	1.2×10^{-4}
	323.40	3.20	0.65	0.55	5×10^{-6}
Polymer 43					
α -process	321.00	2.8	0.35	0.50	2×10^{-6}
	302.22	1.22	0.53	0.53	1×10^{-2}
β_s -process	144.90	0.23	0.38	0.48	2×10^{-2}
β_m -process	236.70	0.55	0.35	0.45	2×10^{-4}

O

||

C

(CH₂)₆

|

CH

O

||

C

O

-

(CH₂)₆

-

O

main chain mesogen

O

-

(CH₂)₆

-

O

side group mesogen

O

-

CH₂

-

CH

-

CH₂

-

CH₃

CH₃

|

CH

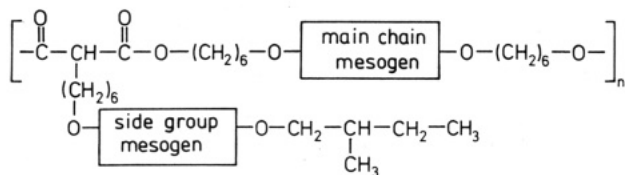


Figure 1. Molecular structure of the investigated combined chain side-group polymers. The main-chain and the side-group mesogens are shown in Table I.

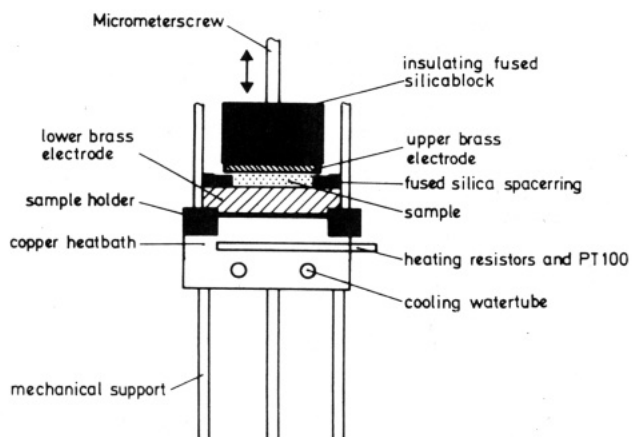


Figure 2. Heating stage inside the vacuum chamber for the bubble free preparation of the samples inside the condenser. The upper electrode is removable via a vacuumlike micrometer screw from the outside.

and $c_2 = 31.6$. At low frequencies the DSC glass transition temperature, indicated by the dashed line, is approached.

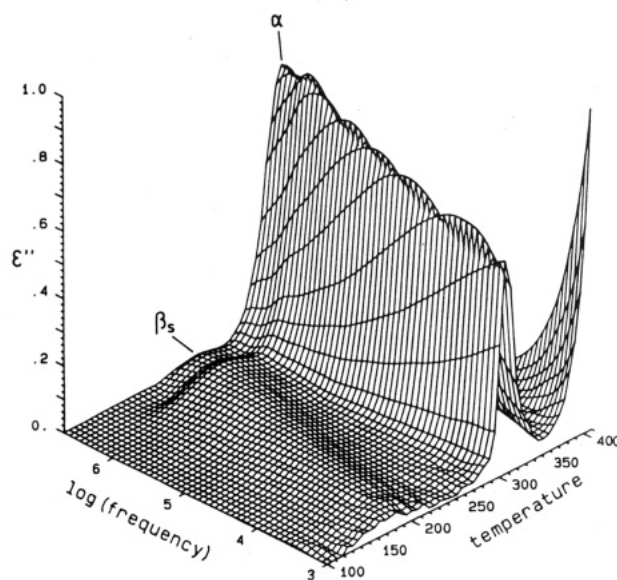


Figure 3. Polymer 29: dielectric loss versus frequency and temperature.

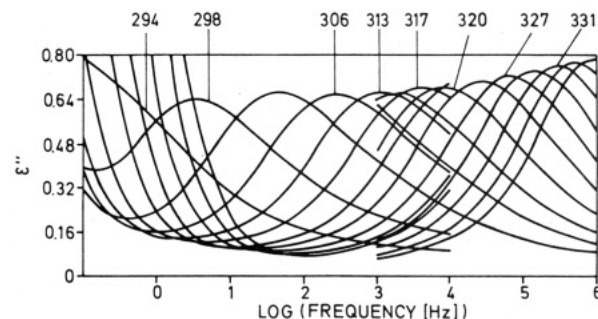


Figure 4. Frequency dependence of the dielectric loss for polymer 29 in the temperature range 294–340 K. Error of measurement, $\pm 5\%$.

Thereby this process is assigned to the α -relaxation process, the dynamic glass process of the polymeric main chain.

From the systematic comparison of the α -process of the four polymers 29, 31, 37, and 39, it can be seen that the mesogenic 3-bromobiphenyl group with a lateral dipole moment contributes to this relaxation by being attached to the main chain as well as to the side group. For example, polymer 31 with a different main-chain mesogen

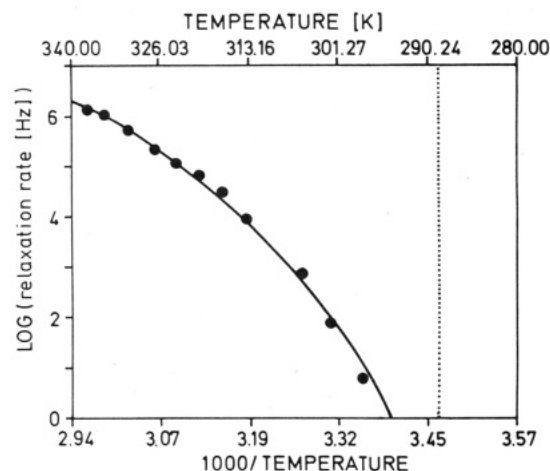


Figure 5. Mean relaxation rate ν_r (determined by fitting the experimental data with the Havriliak-Negami function) versus inverse temperature (WLF plot). The error bars in this and the following figures are not larger than the size of the symbols. The dotted line represents the DSC-determined glass transition temperatures. The drawn line indicates the WLF fit with the parameters: $\log \tau_{T_g} = -1.99$, $c_1 = 13.55$, and $c_2 = 31.56$.

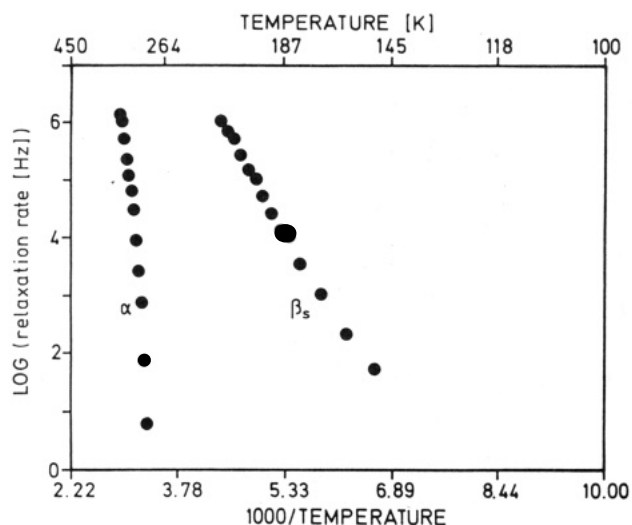


Figure 6. Activation diagram for polymer 29. All mean relaxation rates were determined by fitting the experimental data with the Havriliak-Negami function (also in Figure 8).

(azoxybenzyl) and polymer 37 with a different side-group mesogen (azoxybenzyl) both show a decreased relaxational strength of the α -process. Hence, polymer 39 with the azoxybenzyl mesogen in the main chain as well as in the side group reveals the lowest relaxational strength of all four polymers. Thus, the spacer containing six methylene groups does not fully decouple the glass relaxation of the main chain from the movements of the side groups. This is supported by the parallel arrangement of main-chain and side-group mesogens.^{17,18}

The low-temperature process observed for polymer 29 is strongly asymmetric. This relaxation occurs in all nine polymers at a similar temperature and frequency range. It is assigned to the rotational movement of the mesogenic side group around its long axis (in the following called β_s). This assignment is supported both by a comparison of the relaxational strengths and the activation energies. For the 3-bromobiphenyl group with a stronger steric hindrance and a larger movement of inertia (compared to the azoxybenzyl group), an activation energy of about 39 ± 4 kJ/mol is found (with the azoxybenzyl group 26–30 kJ/mol). Figure 6 shows the activation diagram (i.e., mean relaxation rate ν_r deduced by the Havriliak-Negami

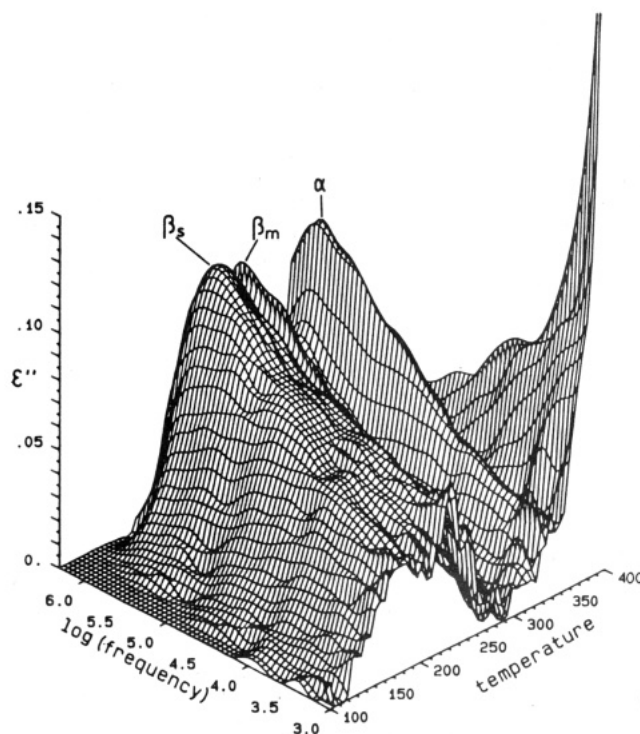


Figure 7. Polymer 40: Dielectric loss versus frequency and temperature.

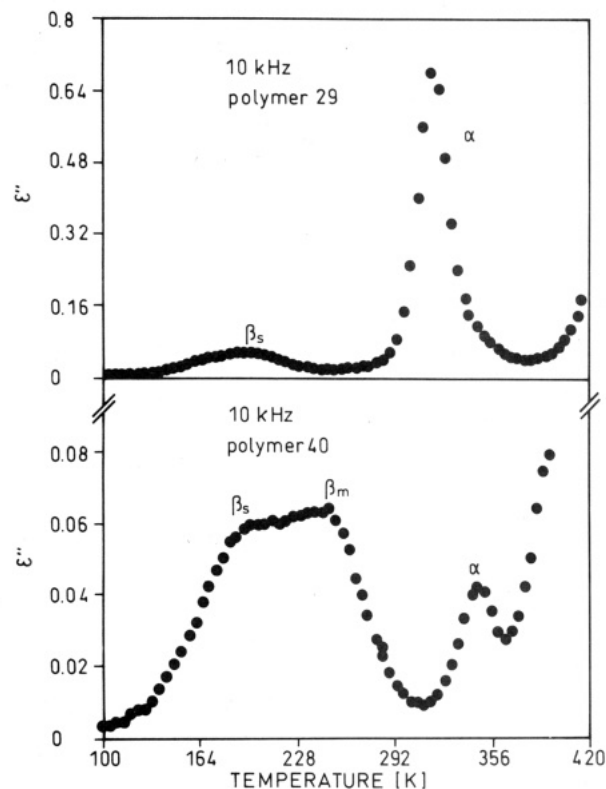


Figure 8. Isochronal ϵ'' versus temperature for polymer 29 and polymer 40 at a frequency of 10 kHz. (Note the different scales in ϵ'' .)

function versus inverse temperature) for the α -process and the β_s -process for polymer 29. A δ -relaxation⁴ was not found, presumably because of the small dipole moment of the terminal moiety in the side group. Replacing this group by the cyano group increases strongly its relaxational strength as shown for homopolymers.²

Polymer 40 (k 77 s^* , 126 s_A 131 i). The polymers with a transition crystalline/lc phase at higher temperatures

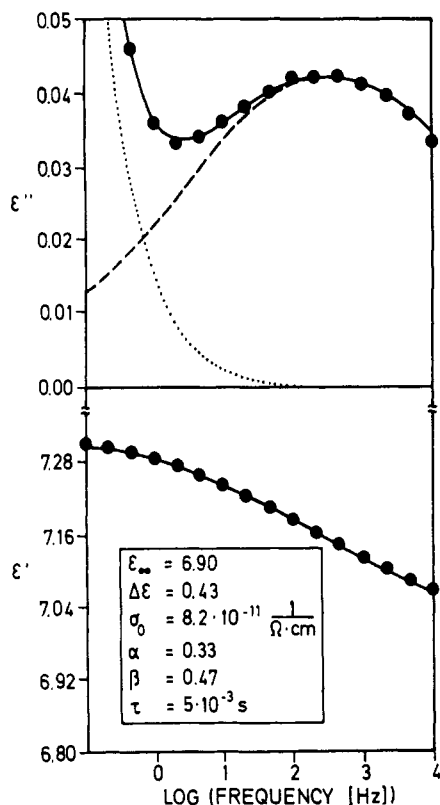


Figure 9. Dots correspond to the experimental values. The dotted line shows the conductivity contribution (according to eq 3); the dashed line shows the relaxation process according to the Havriliak-Negami function (eq 1), using the fit parameters given in the inset. The solid line represents the superposition of both contributions for ϵ'' and ϵ' . The conductivity contribution in ϵ' is obviously negligible.

show different relaxational processes. In Figures 7 and 8, for polymer 40, the dielectric loss is shown at radio frequencies as a function of temperature and frequency. At low frequencies and high temperatures, the contribution of conduction occurs. Its frequency dependence obeys the following equation (19) and can thereby be subtracted, Figure 9.

$$\epsilon''(\omega) = \frac{\sigma_0}{\epsilon_0 \omega (1-s)} \quad (3)$$

ϵ_0 is the permittivity of the free space. σ_0 and s are fit parameters. For s , values of about 0.8 are found, which indicates a hopping conductivity. Besides this contribution, three relaxational processes occur, as can be seen from the three-dimensional representation of the dielectric loss ϵ'' (Figure 7). The relaxational strengths of all three processes is strongly temperature dependent. For the two low-temperature relaxations (β_s , β_m), this is caused by the fact that the relaxational rates at higher frequencies (10^5 – 10^6 Hz) approach each other and hence their relaxational strengths add up. In contrast to this is the decrease of the relaxational strength of the α -process with decreasing frequency and temperature, presumably due to the onset of crystallization within the sample. The activation energies of the β_s -relaxation (i.e., rotation of the mesogenic side group around its long axis) for the different mesogenic groups have comparable values (30–40 kJ/mol) for the crystalline as well as for the amorphous polymers. The temperature dependence of the relaxation rate ν , follows the Arrhenius law over the whole measured frequency range. Since no lateral dipole moment exists within the biphenyl mesogenic group (polymer 41, 43, 44), the ether oxygens, which have an angular dipole moment of

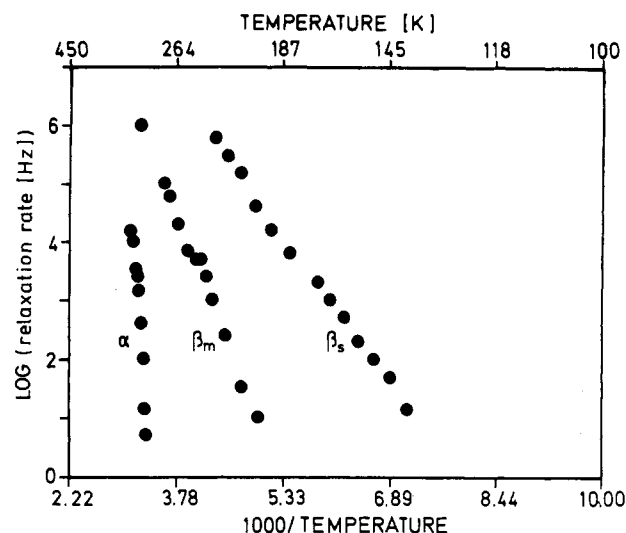


Figure 10. Activation diagram for polymer 43. (All mean relaxation rates were determined by fitting the experimental data with the Havriliak-Negami function.) Polymer 43 was chosen instead of polymer 40 for the activation plot, since the relaxational strength of the α -process of polymer 40 (see Figure 7) decreases so strongly that the numerical analysis was possible only with large uncertainty.

1.28 D,²⁰ make this rotation dielectrically observable. The whole process might be well-compared to the β -process in liquid-crystal side-group polymers.

A new process between these two processes is found on the frequency and temperature scale (Figures 7 and 8). It has an activation energy for the polymers with biphenyl and azoxybenzyl group in the main chain of ca. 55–70 kJ/mol, whereas for polymer 41 with the 3-bromobiphenyl group as mesogen in the main chain a value of 100 ± 4 kJ/mol is found. These values lead to the assignment of this process to the rotational motion of the main-chain mesogen around its long axis. It is called β_m in the following. The separation of the two β -processes increases with decreasing frequency. Since the Havriliak-Negami fit parameters reveal themselves as only slightly temperature dependent, it was possible to fit the data with two broadened and asymmetric relaxation processes at lower frequencies. This was then also possible for two overlapping processes at higher frequencies. In Figure 10 the activation diagram for polymer 43 is shown with the three observed processes: α , β_s , and β_m . In Figure 11 the assignment of the three observed relaxation processes to molecular movements is schematically shown.

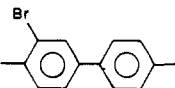
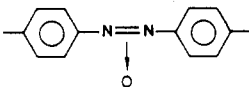
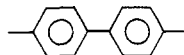
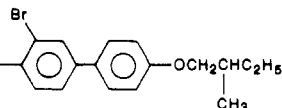
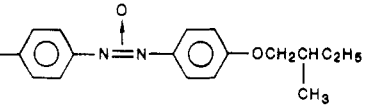
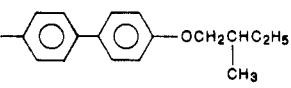
In all above-described experiments, unaligned samples were used. No attempt was tried to make homogeneously and homotropically aligned samples in order to determine the anisotropy of the dielectric function as analyzed in detail by Attard²¹ and Araki et al.²² Using a thin (10 μ m) surface-stabilized LCD cell we could orientate polymer 40 by means of a strong electric field (35 000 V/cm) in the bookshelf geometry. That enabled us to find the two ferroelectric modes (Goldstone and soft mode) as predicted by ref 23. A detailed publication on these nonlinear properties of the s^* phase in polymer 40 is in press.²⁴

Conclusion

The combined main-chain side-group liquid-crystalline polymers show three relaxational processes (see Table III).

α -Process. This occurs in the four glassy polymers and in the crystalline samples. For the latter it has a strongly temperature-dependent strength. It is assigned to the dynamic glass process of the polymeric main chain via spacers coupled side-group movements. The main relax-

Table III
Overview of All Observed Relaxational Processes^a

side-group mesogen	main-chain mesogen		
			
	29: g 12 s 37 i α -process: $c_1 = 13.5$; $c_2 = 31.5$ $\log \tau_{T_g} = -1.99$, $\Delta\epsilon = 3.2$ β_s : $E_a = 39 \pm 4$ kJ/mol, $\Delta\epsilon = 0.45$ β_m : beneath α -process	31: g 12 s 53 n* 91 i α -process: $c_1 = 16.9$; $c_2 = 36.6$ $\log \tau_{T_g} = -2.99$, $\Delta\epsilon = 2.9$ β_s : $E_a = 38 \pm 4$ kJ/mol, $\Delta\epsilon = 0.38$ β_m : beneath α -process	32: k 84 i; i 80 lc ₁ 74 lc ₂ 66 k α -process: $\Delta\epsilon = 1.6$ β_s : $E_a = 32.8$ kJ/mol, $\Delta\epsilon = 0.21$
	37: g 17 s 80 n 96 i α -process: $c_1 = 11.8$; $c_2 = 24.7$ $\log \tau_{T_g} = -0.99$, $\Delta\epsilon = 1.7$ β_s : $E_a = 26 \pm 4$ kJ/mol; $\Delta\epsilon = 0.20$ β_m : beneath α -process	39: g 20 s _A 108 n* 144 i α -process: $c_1 = 8.8$; $c_2 = 13.0$ $\log \tau_{T_g} = -1.69$, $\Delta\epsilon = 1.25$ β_s : $E_a = 30 \pm 4$ kJ/mol, $\Delta\epsilon = 0.21$ β_m : $E_a = 55 \pm 4$ kJ/mol, $\Delta\epsilon = 0.37$	40: k 77 s _c * 126 s _A 131 i α -process: $\Delta\epsilon = 1.6$ β_s : $E_a = 35 \pm 4$ kJ/mol, $\Delta\epsilon = 0.32$ β_m : $E_a = 67 \pm 4$ kJ/mol
	41: k 59 s _c * 105 i α -process: $\Delta\epsilon = 1.8$ β_s : $E_a = 38 \pm 4$ kJ/mol, $\Delta\epsilon = 0.32$ β_m : $E_a = 99 \pm 4$ kJ/mol, $\Delta\epsilon = 0.28$	43: k 63 s _c * 124 n* 133 i α -process: $\Delta\epsilon = 1.3$ β_s : $E_a = 28 \pm 4$ kJ/mol, $\Delta\epsilon = 0.24$ β_m : $E_a = 69 \pm 4$ kJ/mol	44: k ₁ 151 k ₂ 154 i no α -process β_s : $E_a = 32 \pm 4$ kJ/mol, $\Delta\epsilon = 0.34$ no β_m -process

^a $\Delta\epsilon$ is the relaxational strength as defined by $\Delta\epsilon = \epsilon_s - \epsilon_\infty$ and determined by the Havriliak-Negami fit. E_a = activation energy. $\Delta\epsilon$ for the α -process of polymers 40, 41, 43, and 32 were deduced from the temperature dependence of ϵ' at a frequency of 10^6 Hz. This procedure was employed for these four samples, because of the strong temperature dependence of the relaxational strength. (Discussed in detail for polymer 40 in the text.)

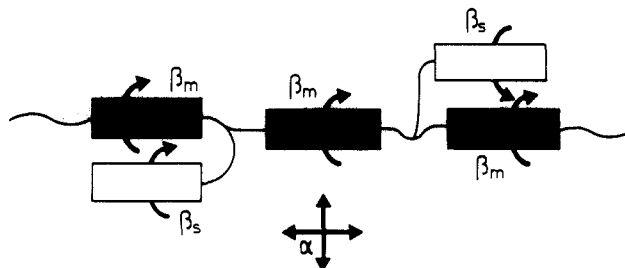


Figure 11. Scheme of the assigned movements inside the liquid-crystalline polymers to the observed relaxation processes.

ation rate can be described by the WLF equation. This process depends on the free volume.

β_s -Process. This occurs in the temperature range from 150 to 250 K and is assigned to the rotation of the mesogenic side group around its long axis. The temperature dependence of the activation energy follows the Arrhenius law. The activation energy has a value of about 30 kJ/mol for the azoxybenzyl and the biphenyl mesogenic group. For the 3-bromobiphenyl group, a value of ca. 38 kJ/mol was found, arising from the larger steric hindrance and the larger moment of inertia. This process was found for all polymers in the glassy state as well as in the crystalline state.

β_m -Process. This can be found in the temperature range 220–270 K and is assigned to the rotation of the mesogenic group in the main chain around its long axis. For the polymers with a lower glass-transition temperature, this process is covered by the stronger α -process. The temperature dependence of the mean relaxation rate is Arrhenius-like. An activation energy of ca. 60 kJ/mol is found for the azoxybenzyl and the biphenyl group, whereas the 3-bromobiphenyl group has a value of ca. 100 kJ/mol.

In Figure 11 the assignment of the three observed relaxation processes to molecular movements is schematically shown.

Acknowledgment. We thank Prof. Dr. E. W. Fischer and Dr. B. Stoll for helpful discussions. The technical assistance of G. Zak and the support in programming the VAX-750 for the three-dimensional representation of the dielectric loss from J. Fittinghoff, Dr. V. Macho, A. Zetsche, and D. Sengelhoff is highly acknowledged.

Registry No. 29 (SRU), 121268-25-5; 29 (copolymer), 121231-73-0; 31 (SRU), 117744-68-0; 31 (copolymer), 121328-15-2; 32 (SRU), 121231-71-8; 32 (copolymer), 121231-74-1; 37 (SRU), 121268-27-7; 37 (copolymer), 121328-18-5; 39 (SRU), 117744-74-8; 39 (copolymer), 121328-19-6; 40 (SRU), 117744-71-5; 40 (copolymer), 121328-17-4; 41 (SRU), 121268-26-6; 41 (copolymer), 121231-75-2; 43 (SRU), 117744-70-4; 43 (copolymer), 121328-16-3; 44 (SRU), 107934-27-0; 44 (copolymer), 107934-44-1.

References and Notes

- Reck, B.; Ringsdorf, H. *Makromol. Chem. Rapid Commun.* **1985**, *6*, 291.
- Endres, B. W.; Wendorff, J. H.; Reck, B.; Ringsdorf, H. *Makromol. Chem.* **1987**, *188*, 1501.
- Monnerie, L.; Laupretre, F.; Noel, C. *Liq. Cryst.* **1988**, *3*, 1013.
- Zentel, R.; Strobl, G. R.; Ringsdorf, H. *Macromolecules* **1985**, *18*, 960.
- Bormuth, F. J.; Haase, W. *Mol. Cryst. Liq. Cryst.* **1987**, *153*, 207.
- Bormuth, F. J.; Haase, W. *Liq. Cryst.* **1988**, *3*, 881.
- Parneix, J. D.; Njeumo, R.; Legrand, L.; LeBarny, P.; Dubois, J. C. *Liq. Cryst.* **1987**, *2*, 167.
- Attard, G. S.; Williams, G.; Gray, G. W.; Lacey, D.; Gemmel, P. A. *Polymer* **1986**, *27*, 185.
- Attard, G. S.; Moura-Ramos, J. J.; Williams, G. *J. Polym. Sci., Polym. Phys. Ed.* **1987**, *25*, 1099.
- Kresse, H.; Kostromin, S.; Shibaev, V. P. *Makromol. Chem. Rapid Commun.* **1982**, *3*, 509.
- Heinrich, W.; Stoll, B. *Colloid. Polym. Sci.* **1985**, *263*, 895.
- Vallerien, S. U.; Kremer, F.; Böffel, C. *Liq. Cryst.* **1989**, *4*, 79.
- Kapitzka, H.; Zentel, R. *Makromol. Chem.* **1988**, *189*, 1793.
- Pugh, J.; Ryan, J. T. *IEE Conf. Dielectr. Mater., Meas. Appl.* **1979**, *177*, 404.
- Havriliak, S.; Negami, S. *J. Polym. Sci.* **1966**, *C14*, 99.
- Williams, M. L.; Landel, R. F.; Ferry, J. D. *J. Am. Chem. Soc.* **1955**, *77*, 3701.

- (17) Zentel, R.; Schmidt, G. F.; Meyer, J.; Benalia, M. *Liq. Cryst.* **1987**, *2*, 651.
 (18) Voigt-Martin, I. G.; Durst, H.; Reck, B.; Ringsdorf, H. *Macromolecules* **1988**, *21*, 1620.
 (19) Mott, N. F.; Davis, E. A. *Electron Processes in Non Crystalline Materials*, 2nd ed.; Clarendon Press: Oxford, 1979.
 (20) Klingbielt, R. T.; Genova, D. J.; Criswell, T. R.; Van Meter, J. P. *J. Am. Chem. Soc.* **1974**, *96*, 7651.
 (21) Attard, G. S. *Mol. Phys.* **1986**, *58*, 1087.
 (22) Attard, G. S.; Araki, K.; Williams, G. *Br. Polym. J.* **1987**, *19*, 119.
 (23) Le Barny, P.; Dubois, J. C. "The chiral smectic C liquid crystal side chain polymers". In *Side Chain Liquid Crystal Polymers*; McArdle, C. B., Ed.; The Blackie Publ. Gp.: Glasgow, 1988.
 (24) Vallerien, S. U.; Zentel, R.; Kremer, F.; Kapitza, H.; Fischer, E. W. *Macromol. Chem. Rapid Commun.*, in press.

Displacement of Polymers by Displacers. 2. Poly(ethylene oxide) at the Silica Surface

Masami Kawaguchi,* Takehiro Hada, and Akira Takahashi

Department of Industrial Chemistry, Faculty of Engineering, Mie University, 1515 Kamihama-cho, Tsu, Mie 514, Japan. Received December 28, 1988; Revised Manuscript Received March 21, 1989

ABSTRACT: Displacement of preadsorbed poly(ethylene oxide) (PEO) was examined by adding various displacer molecules, such as methyl cellosolve, dioxane, acetone, and benzene, to a nonporous Aerosil 130 silica in carbon tetrachloride, using a FT/IR spectrometer. The displacement behavior was followed by the adsorbed amount of PEO and IR spectra of the sedimented silica on which PEO and displacers are adsorbed. The critical volume fraction ϕ_{cr}^d of displacer was obtained by extrapolation of the displacement isotherm curve to no adsorbed amount of PEO. The magnitude of ϕ_{cr}^d values increases in the order of methyl cellosolve, dioxane, acetone, and benzene. Except for methyl cellosolve, in other displacers, PEO can be adsorbed at the silica surface. The adsorption-free energy parameter, χ_s , of PEO for these displacers can be evaluated by using a relationship derived by Cohen Stuart, Fleer, and Scheutjens. Large evaluated χ_s values mean that PEO molecules are strongly attached to the silica surface via hydrogen bonding between surface silanol groups and the oxygen atoms in the ethyloxy segments of PEO.

Introduction

Displacement of the preadsorbed polymer chains from solid-liquid interfaces by the addition of low molecular weight displacer molecules has been related not only to practical view points, such as steric stabilization of colloidal particles upon desorption of polymer chains and adsorption chromatography, but also to the evaluation of segmental adsorption free energy, $\chi_s kT$, where k is the Boltzmann constant and T is the absolute temperature. The value of the adsorption free energy parameter, χ_s , was defined by Silberberg¹ in 1968

$$\chi_s = \frac{[\epsilon_{2s} - \epsilon_{1s} + \frac{1}{2}(\epsilon_{11} - \epsilon_{22})]}{kT} \quad (1)$$

where the term ϵ represents the binary interacting energy among polymer segments (2), solvent molecules (1), and adsorbent surface (s). The χ_s value relates well to the adsorption strength between polymer segments and adsorbent surface. Actually, evaluating the χ_s value leads to further development in the theoretical works on polymer adsorption and quantitatively predicts the adsorption behavior.

In our previous paper,² we displaced homodisperse polystyrenes (PS) by various displacers at the silica surface. Moreover, we have proposed a simple route for evaluation of the χ_s value, using eq 2 predicted by Cohen Stuart et al.,³ if we select a good combination of two solvents, that is, one behaves as a solvent and another as a displacer:

$$\chi_s^{pd} = \ln \phi_{cr}^d + \chi_{sc} - \lambda_1 \chi^{pd} - (1 - \phi_{cr}^d)(1 - \lambda_1)(\chi^{po} - \chi^{pd} - \chi^{do}) \quad (2)$$

where χ_s^{pd} is the adsorption energy parameter of a polymer segment adsorbing from a displacer molecule, ϕ_{cr}^d is the critical volume fraction of a displacer, χ_{sc} is the critical

adsorption energy parameter (polymer adsorption takes place if the χ_s parameter exceeds the χ_{sc} value), λ_1 is the lattice parameter, and χ^{po} , χ^{pd} , and χ^{do} correspond to the interaction parameter between polymer and solvent (po), polymer and displacer (pd), and displacer and solvent (do), respectively.

In this paper we estimate the χ_s parameter of poly(ethylene oxide) (PEO) in various solvents from the displacement of preadsorbed PEO with a narrow molecular weight distribution at a silica surface by the addition of the solvents using eq 2. Moreover, we will discuss the preferential adsorption of PEO over PS at the silica surface for the competitive and displacement adsorption between two polymers⁴ based on comparison of the χ_s values for PEO and PS.

Experimental Section

Material. A PEO sample having $M_w = 39 \times 10^3$ and polydispersity index $M_w/M_n = 1.07$ was purchased from Tosoh Co. Carbon tetrachloride (CCl_4) used as a solvent was distilled just before use.

Spectroquality benzene, dioxane, acetone, and methyl cellosolve were used as displacers without further purification.

The nonporous Aerosil 130 silica (Degussa A. G., West Germany) used as an adsorbent was cleaned by the same procedure as described previously.⁵

Adsorption and Displacement of PEO. The adsorption isotherm of the PEO sample was determined in a 50-mL stoppered glass centrifuge tube containing 0.16 g of silica and 20 mL of a PEO- CCl_4 solution of known concentration, C_0 . The mixture in the tube was stirred with a magnetic chip for 24 h to attain equilibrium in an incubator controlled at $35 \pm 0.1^\circ C$. The silica suspensions were centrifuged at 3000 rpm for 10 min to sediment the silica using a Kubota KR-200B centrifuge, and the supernatant was carefully withdrawn. The concentration of unadsorbed PEO remaining in the supernatant solution was determined from an